RIMS-1749

A numerical verification method for solutions of initial value problems for ODEs using a linearized inverse operator

By

Takehiko KINOSHITA, Takuma KIMURA,
and Mitsuhiro T. NAKAO

June 2012

京都大学　数理解析研究所

RESEARCH INSTITUTE FOR MATHEMATICAL SCIENCES
KYOTO UNIVERSITY, Kyoto, Japan

RIMS Preprints manuscript No. 1749

A numerical verification method for solutions of initial value problems for ODEs using a linearized inverse operator

Takehiko Kinoshita · **Takuma Kimura** · **Mitsuhiro T. Nakao**

June 7, 2012

Abstract We propose a new verification method to enclose solutions for initial value problems of systems of first-order nonlinear ordinary differential equations (ODEs) using a linearized inverse operator. The proposed approach can verify the existence and local uniqueness of the exact solution independent of the choice of the approximation scheme, while the existing methods usually depend on the numerical scheme for the approximate solution. In contrast, most of the well-known verification methods to enclose solutions for nonlinear ODEs work only on the specified approximate solution. Namely, in the existing verification methods the numerical scheme for computing an approximate solution is essentially limited to the Taylor method . Therefore, one of our purposes is to develop a verification method that can obtain guaranteed error bounds independent of the approximation scheme. We will present numerical examples of the proposed verification method that obtain rigorous error bounds of the approximate solutions obtained by the Euler method or the second-order Runge-Kutta method.

Keywords Nonlinear ODEs · Initial Value Problems · Finite Difference Method · Finite Element Method · Numerical Verification Method

Mathematics Subject Classification (2000) 34A34 · 65L05 · 65L12 · 65L60 · 65G20

1 Introduction

In this paper, we consider a numerical verification method for the existence and the local uniqueness of solutions for the following system of first-order nonlinear ordinary differential

Takehiko Kinoshita
Research Institute for Mathematical Sciences, Kyoto University, Kyoto 606-8502, Japan
E-mail: kinosita@kurims.kyoto-u.ac.jp

Takuma Kimura
JST CREST / Faculty of Science and Engineering, Waseda University, Tokyo 169-8555, Japan
E-mail: tkimura@aoni.waseda.jp

Mitsuhiro T. Nakao
Sasebo National College of Technology, Nagasaki 857-1193, Japan
E-mail: mtnakao@post.cc.sasebo.ac.jp

equations (ODEs):

$$\begin{cases} Au' = f(t,u), \quad \text{in } J, & \text{(1a)} \\ u(0) = u_0, & \text{(1b)} \end{cases}$$

where $u := (u_1, \ldots, u_n)^T$ is an n-dimensional vector function. Here, $J := (0,T) \subset \mathbb{R}$, $(T < \infty)$ is a bounded interval, n is a positive integer, A is a symmetric positive-definite matrix in $\mathbb{R}^{n\times n}$, u_0 is an arbitrary initial vector in a given initial-value set $U_0 \subset \mathbb{R}^n$, and f is a nonlinear operator from $J \times L^p(J)^n$ to $L^2(J)^n$, $(2 \le p \le \infty)$. In addition, we assume that f is Fréchet differentiable at an arbitrary $v \in H^1(J)^n$ and the derivative $f'(v)$ belongs to $L^\infty(J)^{n\times n}$. We denote that the solution $u(t)$ of (1a) and (1b) as $u(t;u_0)$. An orbit of (1a) starting at u_0 is given by the set $\gamma(u_0) := \left\{u(t;u_0) \in \mathbb{R}^n \ ; \ t \in \overline{J}\right\}$, where $\overline{J} := [0,T]$ means the closure of J. Moreover, we define the family of the orbit of (1a) and (1b) as the union of the orbits for all initial values, i.e., $\gamma(U_0) := \cup_{u_0 \in U_0} \gamma(u_0)$.

Many methods have been developed for the same purpose. The Lohner method [6] and the Taylor model developed by Berz and Makino [1] are especially well known. Moreover, various software packages exist, including AWA by Lohner [7] and COSY INFINITY by Makino [8]. RiOT and ACETAF by Eble [2] are also available. A technique combining the Taylor model [1] and Nakao's method was proposed by Yamamoto and Komori [11]. All of these existing works are verification methods for the orbits of nonlinear ODEs that use the Taylor series. Therefore, the nonlinear operator f must be smooth enough for t and u.

In contrast, our method is based on functional analysis, and it does not need the higher-order derivatives of f. Moreover, we only need an approximate solution, which can be calculated by any algorithm. Therefore, our method can be applied to a much wider range of mathematical problems than those for which previous methods are appropriate. Also, some of the numerical results in Section 8 show that the present approach gives better accuracy than the existing method.

2 Notation and function spaces

In this section, we introduce the function spaces and the projections onto finite-dimensional subspaces that will be used in this paper. Let $L^2(J)$ be the set of square integrable functions on J, which is a real Hilbert space with inner product $(u,v)_{L^2(J)} := \int_J u(t)v(t)\,dt$. For arbitrary $1 \le q < \infty$, let $L^q(J)$ be a Banach space with norm $\|u\|_{L^q(J)} := \left(\int_J |u(t)|^q \, dt\right)^{\frac{1}{q}}$. Similarly, let $L^\infty(J)$ be a Banach space with norm $\|u\|_{L^\infty(J)} := \operatorname{ess\,sup}_{t\in J} |u(t)|$. For each $u \in L^q(J)^n$, we define $N_q(u) \in \mathbb{R}^n$ as $N_q(u) := \left(\|u_1\|_{L^q(J)}, \ldots, \|u_n\|_{L^q(J)}\right)^T$.

Let $H^1(J)$ be a Sobolev space defined by $H^1(J) := \left\{u \in L^2(J) \ ; \ u' \in L^2(J)\right\}$, which is a Hilbert space with inner product $(u,v)_{H^1(J)} := (u,v)_{L^2(J)} + (u',v')_{L^2(J)}$. Let $V^1(J)$ be a subspace of $H^1(J)$ defined by $V^1(J) := \left\{u \in H^1(J) \ ; \ u(0) = 0\right\}$. Then, $V^1(J)$ is a Hilbert space with inner product $(u,v)_{V^1(J)} := (u',v')_{L^2(J)}$.

For a Banach space X and a positive integer n, we define the n-dimensional Banach space X^n by $X^n := X \times \cdots \times X$ with norm $\|u\|_{X^n} := \sqrt{\sum_{i=1}^n \|u_i\|_X^2}$. Similarly, let $X^{n\times n}$ be an n-by-n matrix Banach space. We denote the $L^\infty(J)^{n\times n}$ norm by $\|B\|_{L^\infty(J)^{n\times n}} := \operatorname{ess\,sup}_{t\in J} \max \sqrt{\sigma\left(B(t)^T B(t)\right)}$, where $\sigma\left(B(t)^T B(t)\right) \subset \mathbb{R}$ are the set of eigenvalues for $B^T B$.

For arbitrary $1 \le q < \infty$, we define the ℓ^q norm for $x \in \mathbb{R}^n$ by $\|x\|_{\ell^q} := \left(\sum_{i=1}^n |x_i|^q\right)^{\frac{1}{q}}$. Moreover, we define the ℓ^∞ norm for $x \in \mathbb{R}^n$ by $\|x\|_{\ell^\infty} := \max\{|x_1|, \ldots, |x_n|\}$.

Let $H_k^1(J)^n$ be a finite-dimensional subspace of $H^1(J)^n$ where $k > 0$ is the discretization parameter.

We denote the set of floating-point numbers by $\mathbb{F}$. For the nonsingular floating-point number matrix $M \in \mathbb{F}^{n\times n}$, the interval vector $[\xi] \subset \mathbb{R}^n$, which includes 0, and the translation vector $\zeta \in \mathbb{F}^n$, we define the initial-value set $U_0 \subset \mathbb{R}^n$ as $U_0 = \zeta + M[\xi]$. Namely, we assume that the initial-value set is represented by an affine map in our verification method.

3 Numerical solutions

From the definition of U_0, ζ is an element of U_0. Therefore, we define $u_k \in H_k^1(J)^n$ as the approximate solution of (1a) and (1b) that approximately satisfies the following nonlinear ODEs:

$$\begin{cases} Au_k' = f(t,u_k), \quad \text{in } J, & \text{(2a)} \\ u_k(0) = \zeta. & \text{(2b)} \end{cases}$$

Namely, it is sufficient to satisfy the equality of (2a) in the approximate sense, but we assume that the equality (2b) is rigorously satisfied. Moreover, we can use any algorithm to solve (2a) numerically. Namely, the calculation to obtain u_k could be done by floating-point number operations, and we do not need any rigorous computations that would yield the exact solution of (2a). However, u_k has to be an element of $H_k^1(J)^n$.

For example, when (2a) and (2b) are solved by the finite difference method, no rounding errors are generated in the calculation of $u_k(0) = \zeta$ because $\zeta \in \mathbb{F}^n$. Therefore, we can consider that the equality (2b) strictly holds. Since the finite difference method provides information only at discrete points of the approximate solution, one has to use some suitable interpolation method to connect between these discrete points. It might be appropriate to choose $H_k^1(J)^n$ as a Lagrange-type finite-element space that has the same order of convergence as the finite difference method.

4 Numerical fundamental matrix of solutions

From the definition of the initial-value set U_0, for an arbitrary initial value $u_0 \in U_0$ there exists $\xi \in [\xi]$ such that $u_0 = \zeta + M\xi$. Here, ζ is the center of U_0, and $M\xi$ is the error for the initial value u_0. In Section 3, we defined the time evolution of ζ in our verification method. In this section, we will define the time evolution for $M\xi$.

Since ξ is the "error", it cannot be strictly expressed in a computer. Therefore, we consider the time evolution of M. Note that ξ is an element of $\mathbb{R}^n$ and is not an interval of $\mathbb{R}^n$. The interval vectors are notated by square brackets, $[\cdot]$, throughout this paper.

Let $E_k \in H_k^1(J)^{n\times n}$ be the approximate fundamental matrix of solutions that satisfies the following linear ODEs:

$$\begin{cases} AE_k' - f'(u_k)E_k = 0 \quad \text{in } J, & \text{(3a)} \\ E_k(0) = M. & \text{(3b)} \end{cases}$$

Notice that, similar to the case of u_k, it is sufficient to approximately satisfy the equality (3a). However, the equality (3b) must be rigorously satisfied. In order to compute E_k, it is usually appropriate to apply the same numerical method as for u_k.

We now define the time evolution of $M\xi$ by $E_k(t)\xi$. Therefore, we can obtain the enclosure of this for any $\xi \in [\xi]$ by $E_k(t)[\xi]$, where $E_k(t)[\xi]$ denotes the multiplication of a matrix and an interval vector.

5 Norm estimates for numerical solutions

In this section, we consider the estimates of E_k. For any $1 \le q \le \infty$ and $i \in \{1,\dots,n\}$, we define $N_q(E_{k,i}) \in \mathbb{R}^n$ by the vector whose elements consist of the $L^q(J)$ norm of the i-th row of E_k, i.e.,

$$N_q(E_{k,i}) := \left(\left\| E_{k,i,1} \right\|_{L^q(J)}, \dots, \left\| E_{k,i,n} \right\|_{L^q(J)} \right)^T.$$

Lemma 5.1 *For any $1 \le q \le \infty$ and $i \in \{1,\dots,n\}$, the following estimate holds:*

$$\sup_{\xi \in [\xi]} \left\| \left(E_k \xi \right)_i \right\|_{L^q(J)} \le \left\| N_q(E_{k,i}) \right\|_{\ell^q} \sup_{\xi \in [\xi]} \left\| \xi \right\|_{\ell^{\frac{q}{q-1}}}. \tag{4}$$

Proof. —— For arbitrary $\xi \in [\xi]$, we set $u_s(t;\xi) := E_k(t)\xi$. Then, the i-th component of u_s is written by $u_{s,i}(t;\xi) = \sum_{j=1}^n E_{k,i,j}(t)\xi_j$.

First, we consider the case of $1 < q < \infty$. From the Hölder inequality, we have

$$\begin{aligned}
\left\| u_{s,i}(\cdot;\xi) \right\|_{L^q(J)}^q &= \int_J \left| \sum_{j=1}^n E_{k,i,j}(t)\xi_j \right|^q dt \\
&\le \int_J \left(\sum_{j=1}^n \left| E_{k,i,j}(t) \right|^q \right) \left(\sum_{j=1}^n \left| \xi_j \right|^{\frac{q}{q-1}} \right)^{q-1} dt \\
&= \left(\sum_{j=1}^n \left\| E_{k,i,j} \right\|_{L^q(J)}^q \right) \left(\sum_{j=1}^n \left| \xi_j \right|^{\frac{q}{q-1}} \right)^{q-1} \\
\left\| u_{s,i}(\cdot;\xi) \right\|_{L^q(J)} &\le \left\| N_q(E_{k,i}) \right\|_{\ell^q} \left\| \xi \right\|_{\ell^{\frac{q}{q-1}}}.
\end{aligned}$$

Next, in the case of $q = 1$, we have

$$\begin{aligned}
\left\| u_{s,i}(\cdot;\xi) \right\|_{L^1(J)} &= \int_J \left| \sum_{j=1}^n E_{k,i,j}(t)\xi_j \right| dt \\
&\le \left(\sum_{j=1}^n \left\| E_{k,i,j} \right\|_{L^1(J)} \right) \max\{|\xi_1|,\dots,|\xi_n|\} \\
&= \left\| N_1(E_{k,i}) \right\|_{\ell^1} \left\| \xi \right\|_{\ell^\infty}.
\end{aligned}$$

Finally, in the case of $q = \infty$, we have

$$\begin{aligned}
\left\| u_{s,i}(\cdot;\xi) \right\|_{L^\infty(J)} &= \operatorname*{ess\,sup}_{t \in J} \left| \sum_{j=1}^n E_{k,i,j}(t)\xi_j \right| \\
&\le \max\left\{ \left\| E_{k,i,1} \right\|_{L^\infty(J)}, \dots, \left\| E_{k,i,n} \right\|_{L^\infty(J)} \right\} \sum_{j=1}^n \left| \xi_j \right| \\
&= \left\| N_\infty(E_{k,i}) \right\|_{\ell^\infty} \left\| \xi \right\|_{\ell^1}.
\end{aligned}$$

Therefore, this proof is completed. □

The upper bounds of $\sup_{\xi \in [\xi]} \left\| \xi \right\|_{\ell^{\frac{q}{q-1}}}$ in the right-hand side of (4) can be computed by interval arithmetic. Note that E_k is approximately computed, but the upper bounds of the norm of E_k must be rigorously computed.

Similarly, the residual norm of $E_k\xi$ is obtained as follows.

Lemma 5.2 *For any $1 \le q \le \infty$ and $i \in \{1,\dots,n\}$, the following estimate holds:*

$$\sup_{\xi\in[\xi]} \left\| \left(\left(AE_k' - f'(u_k)E_k\right)\xi \right)_i \right\|_{L^q(J)} \le \left\| N_q\left(\left(AE_k' - f'(u_k)E_k\right)_i \right) \right\|_{\ell^q} \sup_{\xi\in[\xi]} \|\xi\|_{\ell^{\frac{q}{q-1}}}. \tag{5}$$

The proof is almost the same as that for Lemma 5.1, so we have omitted it.

Since the left-hand side of (5) is the residual norm of $E_k\xi$, we expect that it has a convergence order with respect to the discretization parameter k. However, if we directly compute it by interval arithmetic, the convergence order may not be observed. This phenomenon is considered to be due to the cancellation of significant digits. On the other hand, the estimate of the right-hand side of (5) is separated into the interval $[\xi]$ and the residual norm of E_k, which is independent of $[\xi]$. It plays an essential role in attaining the desired convergence order with respect to the discretization parameter k.

6 Verification conditions of solutions for the residual equation

We defined the approximate solution and the approximate fundamental matrix of solutions in Section 3 and Section 4, respectively. However, the discretization error, the truncation error, and the rounding error of (2a) and (3a) were not considered. We will discuss these errors in the present section using the residual equation.

Let ξ be an arbitrary element of $[\xi]$. Then, the residual equation for ξ is defined by

$$\begin{cases} Aw' - f'(u_k)w = f\left(t, u_k + E_k\xi + w\right) - f'(u_k)w - Au_k' - AE_k'\xi, \text{ in } J, & \text{(6a)} \\ w(0) = 0. & \text{(6b)} \end{cases}$$

From now on, we will denote the right-hand side of (6a) by $g_\xi(w) := f\left(t, u_k + E_k\xi + w\right) - f'(u_k)w - Au_k' - AE_k'\xi$. Moreover, we will denote the solution $w(t)$ of (6a) and (6b) by $w(t;\xi)$. Then, the existence and the local uniqueness of the solution $u(\cdot\,;u_0)$ for (1a) and (1b) are equivalent to the existence and the local uniqueness of the solution $w(\cdot\,;\xi)$ for (6a) and (6b). If we put $u(t;u_0) := u_k(t) + E_k(t)\xi + w(t;\xi)$, then $u(\cdot\,;u_0)$ satisfies (1a). Also, from (2b) and (3b), we obtain the following equality:

$$u(0;u_0) = u_k(0) + E_k(0)\xi + w(0;\xi) = \zeta + M\xi \in U_0.$$

Therefore, in what follows, we consider the existence and the local uniqueness of the solution $w(\cdot\,;\xi)$ for (6a) and (6b).

Let $\mathscr{L}_t : V^1(J)^n \to L^2(J)^n$ be the linear ordinary differential operator of the left-hand side of (6a), i.e., $\mathscr{L}_t := A\frac{d}{dt} - f'(u_k)$. Then, the residual equations (6a) and (6b) are equivalent to the following fixed-point problem:

$$w(\cdot\,;\xi) = \mathscr{L}_t^{-1} g_\xi\left(w(\cdot\,;\xi)\right). \tag{7}$$

We denote the nonlinear integral operator of the right-hand side of (7) by $F_\xi := \mathscr{L}_t^{-1} g_\xi$. Then, from the Sobolev embedding theorem, F_ξ is a compact operator from $L^p(J)^n$ to $L^p(J)^n$. Therefore, we can use the Schauder fixed-point theorem to show the existence of a fixed point of (7).

For a suitable positive constant $\alpha \in \mathbb{R}$, which is independent of ξ but which is determined to be dependent on the interval vector $[\xi]$, we define the candidate set $W_\alpha \subset L^p(J)^n$ as follows:

$$W_\alpha := \left\{ w \in L^p(J)^n \,;\, \|w\|_{L^p(J)^n} \le \alpha \right\}.$$

If W_α satisfies $F_\xi(W_\alpha) \subset W_\alpha$, then at least one fixed point of (7) exists in W_α by the Schauder fixed-point theorem. Therefore, the sufficient condition of $F_\xi(W_\alpha) \subset W_\alpha$ becomes a verification condition for the existence of a solution.

We assume that we can obtain the positive constant C_{L^2,L^p} that satisfies the following estimates:

$$\left\|\mathscr{L}_t^{-1}\right\|_{\mathscr{L}\left(L^2(J)^n, L^p(J)^n\right)} \leq C_{L^2,L^p}. \tag{8}$$

For example, a computational method to get C_{L^2,L^p} is given in [5]. Then, we have the following estimates:

$$\begin{aligned}
\left\|F_\xi(W_\alpha)\right\|_{L^p(J)^n} &= \sup_{w\in W_\alpha} \left\|\mathscr{L}_t^{-1} g_\xi(w)\right\|_{L^p(J)^n} \\
&\leq \left\|\mathscr{L}_t^{-1}\right\|_{\mathscr{L}\left(L^2(J)^n, L^p(J)^n\right)} \sup_{w\in W_\alpha} \left\|g_\xi(w)\right\|_{L^2(J)^n} \\
&\leq C_{L^2,L^p} \sup_{w\in W_\alpha} \left\|g_\xi(w)\right\|_{L^2(J)^n}.
\end{aligned}$$

Therefore, F_ξ-invariance of W_α is written as the the following inequality:

$$C_{L^2,L^p} \sup_{w\in W_\alpha} \left\|g_\xi(w)\right\|_{L^2(J)^n} \leq \alpha. \tag{9}$$

Since the parameter ξ is an arbitrary element of $[\xi]$, we have the sufficient condition of (9) by

$$C_{L^2,L^p} \sup_{\xi\in[\xi]} \sup_{w\in W_\alpha} \left\|g_\xi(w)\right\|_{L^2(J)^n} \leq \alpha. \tag{10}$$

The rigorous upper bounds of supremum for ξ in (10) can be computed by interval arithmetic. Thus, we can obtain the verification condition of the existence for the family of solutions with all initial data in $[\xi]$.

Similarly, we can obtain the verification condition of the local uniqueness for solutions of the residual equation. Let ξ be an arbitrary element of $[\xi] \subset \mathbb{R}^n$. For a suitable positive constant $\gamma \in \mathbb{R}$, if W_γ has F_ξ-contractility, then the fixed point of F_ξ is unique in W_γ. Namely, we show that there exists a constant $0 \leq C_{F_\xi} < 1$ satisfying

$$\left\|F_\xi(w) - F_\xi(\tilde{w})\right\|_{L^p(J)^n} \leq C_{F_\xi} \left\|w - \tilde{w}\right\|_{L^p(J)^n}, \quad \forall w, \tilde{w} \in W_\gamma. \tag{11}$$

Since the parameter ξ is an arbitrary element of $[\xi]$, we have the verification condition, $0 \leq \sup_{\xi\in[\xi]} C_{F_\xi} < 1$, for the local uniqueness of the solution of the residual equation for arbitrary initial data in $[\xi]$.

Remark 6.1 *From the fact that the matrix A is symmetric and positive definite, it is seen that the initial value problems* (1a) *and* $u' = A^{-1} f(t,u)$ *are equivalent. Therefore, without loss of generality, we may assume that A is an identity matrix. However, from our experience on the estimates of the linearized inverse operator [5], the estimates of the inverse of* $A\frac{d}{dt} - f'(u_k)$ *are usually easier than the estimates of the inverse of* $\frac{d}{dt} - A^{-1} f'(u_k)$*. This is because in the estimates for the inverse of* $A\frac{d}{dt} - f'(u_k)$*, it is sufficient to get a lower bound of the minimum eigenvalue of A, while we need the square of the minimum eigenvalue of A for the estimate of the inverse of* $\frac{d}{dt} - A^{-1} f'(u_k)$*.*

7 A posteriori estimates

After verifying the existence of a fixed point of (7), we calculate the a posteriori (error) estimates for the fixed point (i.e., the solution of (6a) and (6b)).

Theorem 7.1 *Let α be a positive constant satisfying* (10)*. For an arbitrary initial value $u_0 \in U_0$, we denote the solution of* (1a) *and* (1b) *by $u(\cdot\,;u_0) \in H^1(J)^n$. Then, for any $1 \le q \le \infty$ and $i \in \{1,\dots,n\}$, we have the following error estimate:*

$$\sup_{u_0 \in U_0} \left\| u_i(\cdot\,;u_0) - u_{k,i} \right\|_{L^q(J)^n} \le C_{L^2,L^q} C_{L^2,L^p}^{-1} \alpha + \left\| N_q(E_{k,i}) \right\|_{\ell^q} \sup_{\xi \in [\xi]} \|\xi\|_{\ell^{\frac{q}{q-1}}}. \tag{12}$$

Proof. —— From the definition of U_0, there exists $\xi \in [\xi]$ such that $u_0 = \zeta + M\xi$. Moreover, $w(\cdot\,;\xi)$ exists in W_α, which is the fixed point of (7) for ξ by assumption (10). Therefore, calculating L^q norm for (7), we have

$$\begin{aligned}
\|w_i(\cdot\,;\xi)\|_{L^q(J)} &\le \|w(\cdot\,;\xi)\|_{L^q(J)^n} \\
&= \left\| \mathscr{L}_t^{-1} g_\xi\left(w(\cdot\,;\xi)\right) \right\|_{L^q(J)^n} \\
&\le C_{L^2,L^q} \left\| g_\xi\left(w(\cdot\,;\xi)\right) \right\|_{L^2(J)^n} \\
&\le C_{L^2,L^q} \sup_{\xi \in [\xi]} \sup_{w \in W_\alpha} \left\| g_\xi(w) \right\|_{L^2(J)^n} \\
&\le C_{L^2,L^q} C_{L^2,L^p}^{-1} \alpha.
\end{aligned}$$

From the fact that $u(t;u_0) = u_k(t) + E_k(t)\xi + w(t;\xi)$, we have

$$\begin{aligned}
\left\| u_i(\cdot\,;u_0) - u_{k,i} \right\|_{L^q(J)} &\le \|(E_k\xi)_i\|_{L^q(J)} + \|w_i(\cdot\,;\xi)\|_{L^q(J)} \\
&\le C_{L^2,L^q} C_{L^2,L^p}^{-1} \alpha + \left\| N_q(E_{k,i}) \right\|_{\ell^q} \sup_{\xi \in [\xi]} \|\xi\|_{\ell^{\frac{q}{q-1}}},
\end{aligned}$$

where we used Lemma 5.1. □

From the result in Theorem 7.1 with $q = \infty$, we obtain the enclosure of the family of the orbit of (1a) and (1b) as follows:

$$\gamma(U_0) \subset \left\{ u_k(t) + c \in \mathbb{R}^n \,;\, t \in \overline{J},\ |c_i| \le C_{L^2,L^\infty} C_{L^2,L^p}^{-1} \alpha + \left\| N_\infty(E_{k,i}) \right\|_{\ell^\infty} \sup_{\xi \in [\xi]} \|\xi\|_{\ell^1} \right\}. \tag{13}$$

In order to verify solutions for the initial value problem step-by-step in time, it is very important to obtain the enclosure of the range of the family of solutions at T, i.e., the set $\{u(T;u_0) \in \mathbb{R}^n \,;\, u_0 \in U_0\}$. This enclosure is immediately obtained from (13). However, the L^∞ estimates like (13) often cause so-called overestimates. Therefore, the enclosure of $u(T;u_0)$ is computed using a different estimate from the result in Theorem 7.1.

Lemma 7.2 *Let α be a positive constant satisfying* (10)*. For arbitrary initial data $\xi \in [\xi]$, we denote the fixed point of* (7) *by $w(\cdot\,;\xi) \in W_\alpha$. Then, for each $i \in \{1,\dots,n\}$, we have the following estimate:*

$$\left| \left(Aw(T;\xi) \right)_i \right| \le \left(\left\| f_i'(u_k) \right\|_{L^{\frac{p}{p-1}}(J)^n} + \sqrt{|J|} C_{L^2,L^p}^{-1} \right) \alpha. \tag{14}$$

Proof. —— From the assumption, the fixed point $w(\cdot;\xi)$ satisies (6a) and (6b). Therefore, from (6a) and (6b), we have

$$\begin{aligned} Aw(T;\xi) &= \int_0^T \frac{d}{dt} Aw(t;\xi)\, dt \\ &= \int_0^T \left(f'(u_k) w(t;\xi) + g_\xi\left(w(t;\xi)\right)\right) dt. \end{aligned}$$

Therefore, we obtain the estimates of the i-th component as follows:

$$\begin{aligned} \left(Aw(T;\xi)\right)_i &= \sum_{j=1}^n \int_0^T f'_{i,j}(u_k) w_j(t;\xi)\, dt + \int_0^T g_{\xi,i}\left(w(t;\xi)\right) dt \\ \left|\left(Aw(T;\xi)\right)_i\right| &\le \sum_{j=1}^n \int_0^T \left|f'_{i,j}(u_k) w_j(t;\xi)\right| dt + \int_0^T \left|g_{\xi,i}\left(w(t;\xi)\right)\right| dt. \end{aligned}$$

From the Hölder inequality and the Schwarz inequality, we have

$$\begin{aligned} \left|\left(Aw(T;\xi)\right)_i\right| &\le \sum_{j=1}^n \left\|f'_{i,j}(u_k)\right\|_{L^{\frac{p}{p-1}}(J)} \left\|w_j(\cdot;\xi)\right\|_{L^p(J)} + \sqrt{|J|}\left\|g_{\xi,i}\left(w(\cdot;\xi)\right)\right\|_{L^2(J)} \\ &\le \left\|f'_i(u_k)\right\|_{L^{\frac{p}{p-1}}(J)^n} \left\|w(\cdot;\xi)\right\|_{L^p(J)^n} + \sqrt{|J|}\left\|g_\xi\left(w(\cdot;\xi)\right)\right\|_{L^2(J)^n}. \end{aligned}$$

Here, $\|w(\cdot;\xi)\|_{L^p(J)^n} \le \alpha$ follows from $w(\cdot;\xi) \in W_\alpha$. Moreover, from (10), we have

$$\left\|g_\xi\left(w(\cdot;\xi)\right)\right\|_{L^2(J)^n} \le \sup_{\xi\in[\xi]} \sup_{w\in W_\alpha} \left\|g_\xi(w)\right\|_{L^2(J)^n} \le C^{-1}_{L^2,L^p}\alpha.$$

Therefore, we obtain

$$\left|\left(Aw(T;\xi)\right)_i\right| \le \left\|f'_i(u_k)\right\|_{L^{\frac{p}{p-1}}(J)^n} \alpha + \sqrt{|J|} C^{-1}_{L^2,L^p}\alpha,$$

which completes the proof. □

Let $[r_W] \subset \mathbb{R}^n$ be an interval vector such that each component is defined by

$$[r_{W,i}] := \left[-\left\|f'_i(u_k)\right\|_{L^{\frac{p}{p-1}}(J)^n} - \sqrt{|J|}C^{-1}_{L^2,L^p}, \left\|f'_i(u_k)\right\|_{L^{\frac{p}{p-1}}(J)^n} + \sqrt{|J|}C^{-1}_{L^2,L^p}\right]\alpha.$$

Then, the results of Lemma 7.2 show that the range of $Aw(T;\cdot)$ is included in $[r_W]$, i.e., $\bigcup_{\xi\in[\xi]} Aw(T;\xi) \subset [r_W]$. Let $[\eta]$ be an interval vector in $\mathbb{R}^n$ defined by

$$[\eta] := [\xi] + E_k(T)^{-1}A^{-1}[r_W]. \tag{15}$$

We have an enclosure of the range of u using $[\eta]$ as follows.

Theorem 7.3 *Under the same assumptions as in Theorem 7.1, we have the following enclosure:*

$$\bigcup_{u_0\in U_0} u(T;u_0) \subset u_k(T) + E_k(T)[\eta]. \tag{16}$$

Proof. —— From the assumptions, for arbitrary $u_0 \in U_0$ there exists $\xi \in [\xi]$ such that $u_0 = \zeta + M\xi$ and $u(t;u_0) = u_k(t) + E_k(t)\xi + w(t;\xi)$. From Lemma 7.2, we have

$$\begin{aligned} u(T;u_0) &= u_k(T) + E_k(T)\xi + w(T;\xi) \\ &= u_k(T) + E_k(T)\big(\xi + E_k(T)^{-1}A^{-1}Aw(T;\xi)\big) \\ &\in u_k(T) + E_k(T)\big([\xi] + E_k(T)^{-1}A^{-1}[r_W]\big). \end{aligned}$$

Therefore, this proof is completed. □

Remark 7.4 (Wrapping effect) *When we verify a family of the orbits of the initial value problems step-by-step in time, the so-called* ***wrapping effect*** *appears. The effect is that the validated set exponentially increases with the time variable in the verification process unless a counterplan is considered. Usually, this effect is generated by the interval arithmetic during the multiplication of matrices and vectors. In our verification method, the wrapping effect is mainly generated in the computation of* $[\eta]$*. Therefore, it is necessary to carry out the computation of* $[\eta]$ *using a sufficiently careful technique.*

Lohner proposed a computation technique to reduce the wrapping effect in his method [6]. Note that, for a nonsingular matrix $B \in \mathbb{R}^{n\times n}$, (15) can be rewritten as:

$$[\eta] = B\left(B^{-1}[\xi] + B^{-1}\big(AE_k(T)\big)^{-1}[r_W]\right). \tag{17}$$

Lohner choose B as an approximate orthogonal matrix that appears in the QR decomposition of $\big(AE_k(T)\big)^{-1}$. The following algorithm shows the computational sequence of (17) by Lohner.

Lohner's algorithm [6]
1. $B \leftarrow$ Q factor for numerical QR decomposition of $\big(AE_k(T)\big)^{-1}$
2. $[R] \leftarrow [B^{-1}]\big[\big(AE_k(T)\big)^{-1}\big]$
3. $[\tilde{\eta}] \leftarrow [B^{-1}][\xi] + [R][r_W]$
4. $[\eta] \leftarrow B[\tilde{\eta}]$

From Theorem 7.3, we obtain the set that includes the range of solutions of (1a) and (1b). Moreover, notice that the set of the right-hand side of (16) is given by an affine map. Since the initial value for the next time step is taken as $u_k(T) + E_k(T)[\eta]$, our verification of the solution continues in a step-by-step fashion.

8 Verification results

In this section, we show some results by our verification method for the same problems treated by Yamamoto and Komori [11].

Let A be the identity matrix in $\mathbb{R}^{2\times 2}$. We define the initial ζ by $\zeta = (0,4)^T \in \mathbb{F}^2$ and the initial M as the identity matrix in $\mathbb{R}^{2\times 2}$. We take $[\xi] \subset \mathbb{R}^2$ as a point vector $([0,0],[0,0])^T$ or an interval vector $([-0.05,0.05],[-0.05,0.05])^T$. Let J be an open interval in $\mathbb{R}$ satisfying $|J| = 0.01$, and we try to verify this, step-by-step with step size $|J|$, up to the desired time. In order to solve (2a) and (3a) numerically, we used the Euler method or the second-order Runge-Kutta method (RK2). Note that, in the present case, the equalities of (2b) and (3b)

are strictly satisfied. Corresponding to the Euler method, i.e., first-order accuracy, we used the P1 finite-element space as $H_k^1(J)^2$. Similarly, since RK2 has second-order accuracy, we used the P2 finite-element space in that case. We used a uniform time step with $k = 0.005$ or $k = 0.0005$.

8.1 Linear problem

Now we present the verification results for the solution $u(t;u_0) = \big(u_1(t;u_0), u_2(t;u_0)\big)^T$ of the following linear ODEs with an ending time of 6.28:

$$\begin{cases} u_1' = u_2, & \text{(18a)} \\ u_2' = -u_1. & \text{(18b)} \end{cases}$$

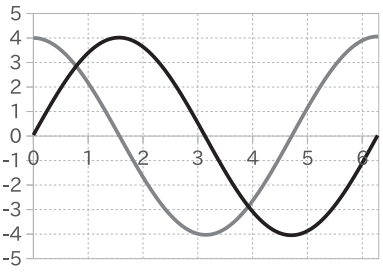

Fig. 1 Graph of $u_{k,1}$ and $u_{k,2}$

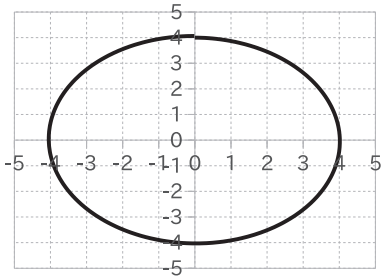

Fig. 2 Phase portrait

Figure 1 shows the approximate solution u_k. The horizontal and vertical axes correspond to time and $u_k(t)$, respectively. Moreover, the black and gray lines show $u_{k,1}$ and $u_{k,2}$, respectively. Figure 2 is the phase plane of u_k.

In this problem, since $n = 2$ and $f(u) = (u_2, -u_1)^T$ is a linear operator, we adopted $L^2(J)^2$ as the basic function space for verification, i.e., we choose $p = 2$. The Fréchet derivative of f at the approximate solution $u_k \in H_k^1(J)^2$ is given by

$$f'(u_k) = \begin{pmatrix} 0 & 1 \\ -1 & 0 \end{pmatrix}.$$

On the other hand, $u_s \in H_k^1(J)^2$ is defined by $u_s := E_k\xi$. Then, the residuals for u_k and u_s are given by $r_e := -u_k' + f(u_k)$ and $s_e := -u_s' + f'(u_k)u_s$, respectively. Therefore g_ξ, which is the right-hand side of the residual equation (6a), is given by

$$g_\xi(w) = \begin{pmatrix} u_{k,2} + u_{s,2} + w_2 - w_2 - u_{k,1}' - u_{s,1}' \\ -(u_{k,1} + u_{s,1} + w_1) + w_1 - u_{k,2}' - u_{s,2}' \end{pmatrix} = \begin{pmatrix} r_{e,1} + s_{e,1} \\ r_{e,2} + s_{e,2} \end{pmatrix}.$$

Next, we consider the sufficient condition of (10). From the linearity of the problem, observe that

$$\begin{aligned} C_{L^2,L^2} \sup_{\xi\in[\xi]} \sup_{w\in W_\alpha} \big\|g_\xi(w)\big\|_{L^2(J)^2} &= C_{L^2,L^2} \sup_{\xi\in[\xi]} \|r_e + s_e\|_{L^2(J)^2} \\ &\le C_{L^2,L^2} \sup_{\xi\in[\xi]} \sqrt{\Big(\|r_{e,1}\|_{L^2(J)} + \|s_{e,1}\|_{L^2(J)}\Big)^2 + \Big(\|r_{e,2}\|_{L^2(J)} + \|s_{e,2}\|_{L^2(J)}\Big)^2}. \end{aligned}$$

Therefore, if the positive constant α is taken as

$$\alpha := C_{L^2,L^2}\sqrt{\left(\|r_{e,1}\|_{L^2(J)} + \sup_{\xi\in[\xi]}\|s_{e,1}\|_{L^2(J)}\right)^2 + \left(\|r_{e,2}\|_{L^2(J)} + \sup_{\xi\in[\xi]}\|s_{e,2}\|_{L^2(J)}\right)^2},$$

then the F_ξ-invariance of W_α is satisfied.

Example 8.1-1: P1 element with $[\xi] = ([0,0],[0,0])^T$

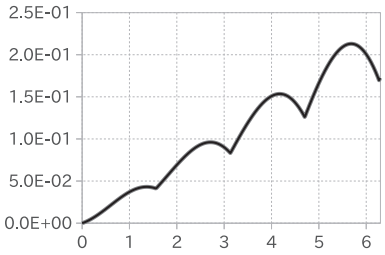

Fig. 3 $k = 0.005$

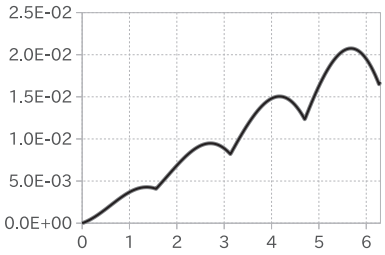

Fig. 4 $k = 0.0005$

Figure 3 and Fig. 4 show the upper bounds of errors for the approximate solution for the P1 element (Euler method) with uniform step size $k = 0.005$ and $k = 0.0005$, respectively. The horizontal axis is the time and the vertical axis corresponds to the error $e_r := \sup_{u_0\in U_0}|u(t;u_0) - u_k(t)|$. Moreover, the black and gray lines show $e_{r,1}$ and $e_{r,2}$, respectively. However, these two lines seem to be almost overlapping in this case.

From the above results, it seems that the errors are increasing in time with order approximately $O(t)$. These results mean that there is no wrapping effect that causes an exponential increase in the validated region. Moreover, the magnitude of errors in Fig. 4 is approximately $\frac{1}{10}$ in Fig. 3. Therefore, we may deduce that our verification algorithm has a convergence order $O(k)$, which seems to be a reasonable result for using the P1 element (Euler method).

Example 8.1-2: P1 element with $[\xi] = ([-0.05,0.05],[-0.05,0.05])^T$

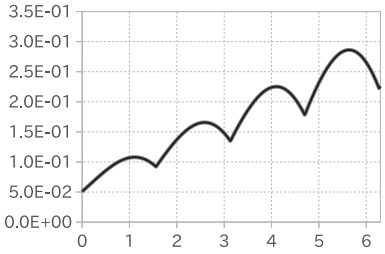

Fig. 5 $k = 0.005$

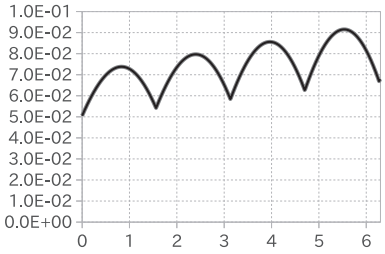

Fig. 6 $k = 0.0005$

Figure 5 and Fig. 6 are the verification results from starting with interval initial data. The increase in the validated region still remains approximately $O(t)$ even if the initial-value set is fairly big.

Example 8.1-3: P2 element with $[\xi] = ([0,0],[0,0])^T$

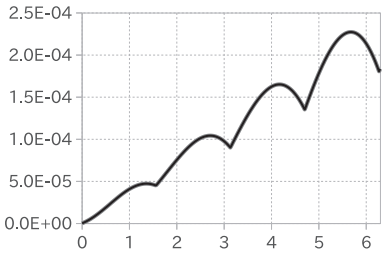

Fig. 7 $k = 0.005$

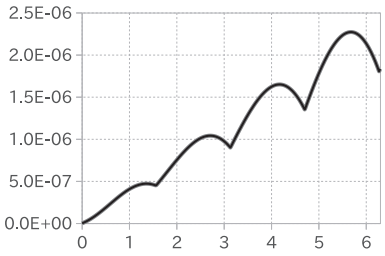

Fig. 8 $k = 0.0005$

Figure 7 and Fig. 8 are the verification results with the P2 element (RK2) and a point initial value. These graphs are also increasing by approximately $O(t)$ in time. Moreover, it seems that our verification algorithm has an accuracy of $O(k^2)$, which is also a quite natural result for the P2 element.

In the present case, since the exact solution of this problem is $u(t;\zeta) = 4(\sin t, \cos t)^T$, we can directly compute the difference between u and u_k. Table 1 shows the actual errors at nodal points and our verification results. As shown in Table 1, the accuracy of our verification results is at most twice the exact error.

Table 1 Exact errors and validated range at nodal points

k	$\max_{1\le j\le 2, 0\le t_i\le 6.28} \lvert u_j(t_i;\zeta) - u_{k,j}(t_i)\rvert$	$\max_{1\le j\le 2, 0\le t_i\le 6.28} e_{r,j}(t_i)$
0.005	1.049910E-04	2.2736E-04
0.0005	1.049858E-06	2.2734E-06

Example 8.1-4: P2 element with $[\xi] = ([-0.05,0.05],[-0.05,0.05])^T$

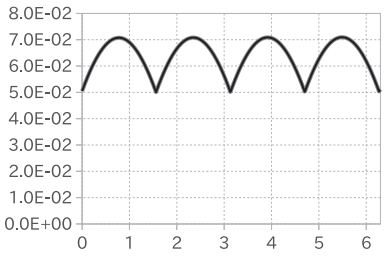

Fig. 9 $k = 0.005$

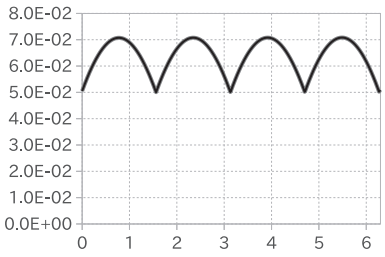

Fig. 10 $k = 0.0005$

Figure 9 and Fig. 10 are the verification results of using the P2 element (RK2) with interval initial data. In this case, it seems that the behavior of the bounds of the validated region is almost independent of the time, for the error bounds are relatively small compared with the width of the interval initial data. The enlargement is at most 10^{-3} for the validated

region in Fig. 9. It is also seen that every graph for this problem repeats the pattern of increasing and decreasing. This phenomenon is due to the fact that the box of the initial-value set leads to a set of closed orbits in the phase space. The length of the diagonal of this box, i.e., $0.05\sqrt{2} \approx 0.07071$, is the maximum value of Fig. 9.

8.2 Nonlinear problem

In this subsection, we show some verification results for the solutions $u(t;u_0) = \big(u_1(t;u_0), u_2(t;u_0)\big)^T$ of the following nonlinear ODEs introduced by Yamomoto and Komori [11]:

$$\begin{cases} u_1' = u_2, & \text{(19a)} \\ u_2' = u_1 - u_1^3. & \text{(19b)} \end{cases}$$

We now show the results until an ending time of 3.3 so that it is the same length as shown by Yamamoto and Komori [11].

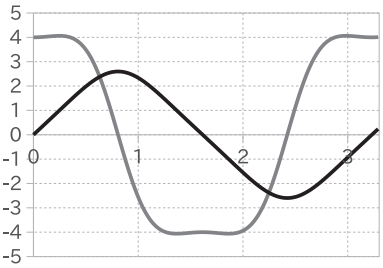

Fig. 11 Graph of $u_{k,1}$ and $u_{k,2}$

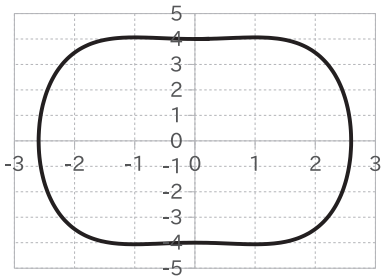

Fig. 12 Phase portrait

Figure 11 is the graph showing the approximate solution u_k. The black and gray lines correspond to $u_{k,1}$ and $u_{k,2}$, respectively. Figure 12 is the phase plane of u_k.

In this problem, due to the fact that $n = 2$ and $f(u) = \big(u_2, u_1 - u_1^3\big)^T$ has cubic nonlinearity, we used the space $L^6(J)^2$, i.e., we choose $p = 6$. The Fréchet derivative of f at the approximate solution $u_k \in H_k^1(J)^2$ is given by

$$f'(u_k) = \begin{pmatrix} 0 & 1 \\ 1 - 3u_{k,1}^2 & 0 \end{pmatrix}.$$

We define $u_s \in H_k^1(J)^2$ by $u_s := E_k\xi$, as before. Also, the residuals for u_k and u_s are defined by $r_e := -u_k' + f(u_k)$ and $s_e := -u_s' + f'(u_k)u_s$, respectively. Then, g_ξ in (6a) is given as follows,

$$\begin{aligned} g_\xi(w) &= \begin{pmatrix} u_{k,2} + u_{s,2} + w_2 - w_2 - u_{k,1}' - u_{s,1}' \\ u_{k,1} + u_{s,1} + w_1 - (u_{k,1} + u_{s,1} + w_1)^3 - (1 - 3u_{k,1}^2)w_1 - u_{k,2}' - u_{s,2}' \end{pmatrix} \\ &= \begin{pmatrix} r_{e,1} + s_{e,1} \\ -(3u_{k,1} + u_{s,1} + w_1)(u_{s,1} + w_1)^2 + r_{e,2} + s_{e,2} \end{pmatrix}. \end{aligned}$$

Next, we consider the condition of (10). Since $g_{\xi,1}$ is not dependent on w, we have

$$\big\|g_{\xi,1}(w)\big\|_{L^2(J)} \le \|r_{e,1}\|_{L^2(J)} + \|s_{e,1}\|_{L^2(J)}.$$

On the other hand, for an arbitrary $w \in W_\alpha$, we get

$$\left\|g_{\xi,2}(w)\right\|_{L^2(J)} \leq \|r_{e,2}\|_{L^2(J)} + \|s_{e,2}\|_{L^2(J)} + \left\|\left(3u_{k,1}+u_{s,1}+w_1\right)\left(u_{s,1}+w_1\right)^2\right\|_{L^2(J)}.$$

Using the Hölder inequality, the third term of the right-hand side is estimated as

$$\begin{aligned}\left\|\left(3u_{k,1}+u_{s,1}+w_1\right)\left(u_{s,1}+w_1\right)^2\right\|_{L^2(J)} &\leq \left\|3u_{k,1}+u_{s,1}+w_1\right\|_{L^6(J)} \left\|u_{s,1}+w_1\right\|^2_{L^6(J)} \\ &\leq \left(3\left\|u_{k,1}\right\|_{L^6}+\|u_{s,1}\|_{L^6}+\alpha\right)\left(\|u_{s,1}\|_{L^6}+\alpha\right)^2.\end{aligned}$$

Therefore, we have

$$\begin{aligned}&\sup_{\xi\in[\xi]}\sup_{w\in W_\alpha}\left\|g_\xi(w)\right\|_{L^2(J)^2} = \sup_{\xi\in[\xi]}\sup_{w\in W_\alpha}\sqrt{\left\|g_{\xi,1}(w)\right\|^2_{L^2(J)}+\left\|g_{\xi,2}(w)\right\|^2_{L^2(J)}} \\ &\leq \sup_{\xi\in[\xi]}\sqrt{\left(\left\|r_{e,1}\right\|_{L^2}+\left\|s_{e,1}\right\|_{L^2}\right)^2+\left(\left\|r_{e,2}\right\|_{L^2}+\left\|s_{e,2}\right\|_{L^2}+\left(\alpha+\|u_{s,1}\|_{L^6}+3\left\|u_{k,1}\right\|_{L^6}\right)\left(\alpha+\left\|u_{s,1}\right\|_{L^6}\right)^2\right)^2}.\end{aligned}$$

From the above, we obtain a sufficient condition for (10), which leads to a sixth-order algebraic inequality in α. Therefore, if we find a positive constant α satisfying this inequality, then it implies the F_ξ-invariance of W_α.

Example 8.2-1: P1 element with $[\xi] = ([0,0],[0,0])^T$

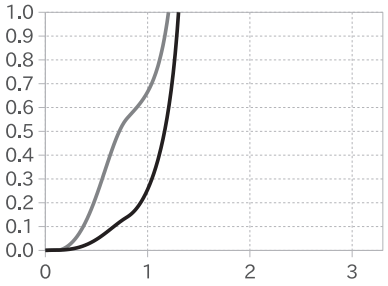

Fig. 13 $k = 0.005$

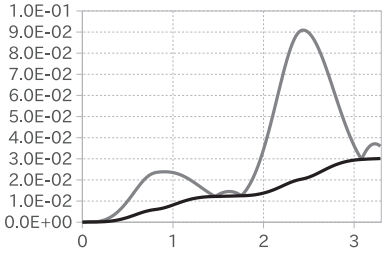

Fig. 14 $k = 0.0005$

Figure 13 and Fig. 14 show the upper bounds of the errors for the approximate solution for the P1 element (Euler method) with uniform step size $k = 0.005$ and $k = 0.0005$, respectively. The horizontal and vertical axes correspond to the time and the error $e_r := \sup_{u_0\in U_0}|u(t;u_0)-u_k(t)|$, respectively. Moreover, the black and gray lines show $e_{r,1}$ and $e_{r,2}$, respectively.

As shown in Fig. 13, in the case of $k = 0.005$, our verification was unsuccessful before $T = 3.3$. On the other hand, by the use of a smaller step size, i.e., $k = 0.0005$, we successfully verified until the desired time. However, as shown in Fig. 14, the verified accuracy seems to be coarse.

Example 8.2-2: P1 element with $[\xi] = ([-0.05,0.05],[-0.05,0.05])^T$

Figure 15 and Fig. 16 are the verification results with interval initial data. In this case, the verifications were not quickly successful.

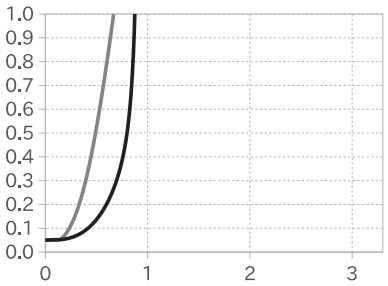

Fig. 15 $k = 0.005$

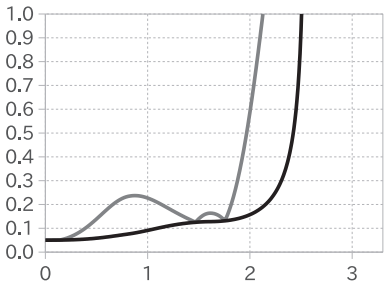

Fig. 16 $k = 0.0005$

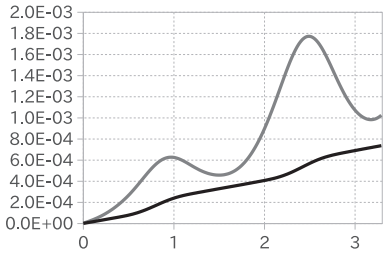

Fig. 17 $k = 0.005$

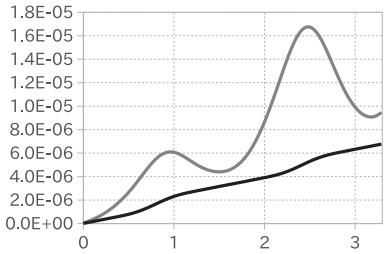

Fig. 18 $k = 0.0005$

Example 8.2-3: P2 element with $[\xi] = ([0,0],[0,0])^T$

Figure 17 and Fig. 18 show the verification results when we used the P2 element (RK2). These results suggest that the accuracy of our verification algorithm is of the order $O(k^2)$.

Example 8.2-4: P2 element with $[\xi] = ([-0.05,0.05],[-0.05,0.05])^T$

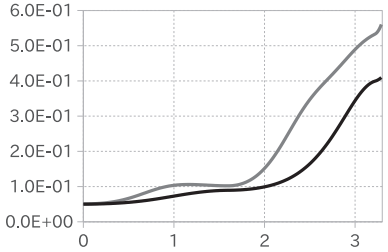

Fig. 19 $k = 0.005$

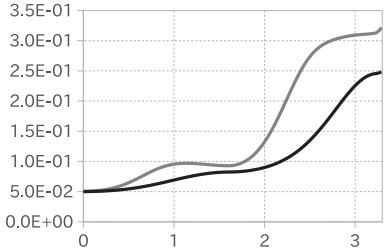

Fig. 20 $k = 0.0005$

Figure 19 and Fig. 20 are the verification results from using the P2 element (RK2) with interval initial data. The validated computations are successful until the desired time $T = 3.3$, but the relative error is not very good.

From these verification results, we can expect that our verification method has the same accuracy as the magnitude of the residual norms $\|r_e\|$ and $\|s_e\|$. When an initial value is the point interval, the order of the validated accuracy seems to be $O(k)$ and $O(k^2)$ with step size k for the P1 and P2 elements, respectively. As a consequence, it is seen that, compared with the numerical examples of Yamamoto and Komori [11], our results are more accurate

in the case of the P2 element but worse for the P1 element. Therefore, in order to attain high-accuracy verification when using our method, we should choose a numerical algorithm that results in a small residual norm.

Remark 8.1 (Computer environment) *All computations were carried out on an Intel Core i7 860, 16GB of DDR3 memory (OS: Windows 7) using INTLAB version 6.0, a toolbox in MATLAB 2010b developed by Rump [10] for self-validating algorithms. Therefore, all numerical values in these tables are verified data in the sense of strict rounding-error control.*

9 Conclusions

We proposed a new verification method to enclose solutions of initial value problems for systems of first-order nonlinear ODEs using a linearized inverse operator. We proved that the wrapping effect could be satisfactorily reduced using an affine map to the initial-value set. If we use the approximate solution with sufficient accuracy, the exponential enlargement of the validated region could be avoided in the verification results. Moreover, the validated accuracy of the proposed method is essentially dependent on the residual norm of the approximate solutions. Therefore, in order to obtain high-accuracy verification, we should choose the numerical algorithm that yields the smallest possible residual norm.

Acknowledgements This work is supported by Grants-in-Aid for Scientific Research (S) 20224001 and (B) 23740074. T. Kinoshita is supported by GCOE 'Fostering top leaders in mathematics', Kyoto University.

References

1. Berz, M., Makino, K.: Verified Integration of ODEs and Flows Using Differential Algebraic Methods on High-Order Taylor Models. Reliab. Comput. 4, 361–369 (1998)
2. Eble, I., Neher, M.: ACETAF: A software package for computing validated bounds for Taylor coefficients of analytic functions. ACM Trans. Math. Software 29, 263–286 (2003)
3. Galias, Z., Zgliczyński, P.: Computer assisted proof of chaos in the Lorenz equations. Phys. D 115, 165–188 (1998)
4. Kimura, S., Yamamoto, N.: On explicit bounds in the error for the H_0^1-projection into piecewise polynomial spaces. Bull. Inform. Cybernet. 31, 109–115 (1999)
5. Kinoshita, T., Kimura, T., Nakao, M.T.: A posteriori estimates of inverse operators for initial value problems in linear ordinary differential equations. J. Comput. Appl. Math. 236, 1622–1636 (2011)
6. Lohner, R.J.: Enclosing the solutions of ordinary initial and boundary value problems. In: Kaucher, C.U.E, Kulish, U. (eds.) Computer Arithmetic: Scientific Computation and Programming Languages, pp. 255–286. Teubner, Stuttgaxt (1987)
7. Lohner, R.J.: Computation of guaranteed enclosures for the solutions of ordinary initial and boundary value problems. In: Computational ordinary differential equations (London, 1989), pp. 425–435. Inst. Math. Appl. Conf. Ser. New Ser., 39, Oxford Univ. Press, New York (1992)
8. Makino, K., Berz, M.: COSY INFINITY Version 9. Nucl. Instr. Meth. Phys. Res. A558, 346–350 (2005)
9. Nakao, M.T., Yamamoto, N., Kimura, S.: On the Best Constant in the Error Bound for the H_0^1-Projection into Piecewise Polynomial Spaces. J. Approx. Theory 93, 491–500 (1998)
10. Rump, S.M.: INTLAB–INTerval LABoratory. In: Csendes, T. (ed.) Developments in Reliable Computing, pp. 77–104. Kluwer Academic Publishers, Dordrecht (1999) http://www.ti3.tu-harburg.de/rump/intlab/
11. Yamamoto, N., Komori, T.: An Application of Taylor Models to the Nakao Method on ODEs. Jpn. J. Ind. Appl. Math. 26, 365–392 (2009)